19

Institute of Theoretical
and Experimental Physics

5-98

FERMILAB
APR 30 1998
LIBRARY

D.G.Koshkarev, A.V.Barkhudaryan, A.N.Talyzin

ITEP-5-98

Fermilab Library
0 1160 0061613 0

New Concept of Charge-Symmetric Driver for Heavy Ion Fusion

Moscow 1998

UDK 621.384 M-16

NEW CONCEPT OF CHARGE-SYMMETRIC DRIVER FOR HEAVY ION FUSION:
Preprint ITEP 4-98/

D.G.Koshkarev, A.V.Barkhudaryan, A.N.Talyzin - M., 1998 - 20p.

First a driver for HIF based on the idea of charge-symmetric beams of some singly charged positive and negative heavy ions was proposed at Frascati HIF Symposium in 1993. The beams of these ions are merged in the final stage of the transport channels in order to reduce the space charge and, therefore, to increase a total particle current on a thermonuclear target. However, for the high beam power and energy getting, the scheme of that driver was rather expensive because of the necessety to use no one, but four ion species and a complex system of storage rings. Now we present a new advanced driver scheme which consept has a specific feature -- the beam bunch structure is maintaining down to the ion beam encounter with the target what allowes to use ions of one element only, to simplify the magnetic rings system, and, as consequence, to avoid the limits on the beam current arising from instabilities and the Lasslet tune shift. As example the driver on base ions Au of the energy 10 GeV are considered. The total driver energy is $\simeq 10MJ$ with peak power about of $2 \cdot 10^{15}$ W.

Fig. - 8, ref. - 8 name.

© Институт теоретической и экспериментальной физики, 1998

1 Introduction

The idea of the charge-symmetric driver was proposed at Frascati HIF Symposium in 1993 [1]. The concept of this driver was based on the acceleration of eight different species of platinum ions (four different isotopes, each in the two states of singly charged positive and negative ions) in the same linear accelerator complex. Negative ion beams are merged with the positive ones in the final stage of the transport channel in order to reduce the space charge and make possible the increase the total particle current on target. The telescopic method was used for different mass ions so that they arrive at the target simultaneously and provide the target irradiation energy of 9.6 MJ and power 960 TW (see [1],[2]). But this scheme was rather complicated and expensive due to the presence of a system of storage and compression rings after linac exit for each ion species.

Now we introduce a simpler scheme of HIF driver based on the idea to maintain the beam bunch structure down to the ion beam encounter with thermonuclear target, which together with new design of the ring system allows to refuse from a telescopic method and to use two ion types only, namely, Au^{+1} and Au^{-1} [3]. The main specifications of this driver are listed in Table 1. A sketch of the driver layout is shown on Fig. 1. The beam parameters at different driver stages are listed in Table 2.

Table 1: Main driver parameters

Ion mass (Au)	Pulse dur. at linac entrance	Ion energy	Pulse dur. at linac exit	Number of irrad. beams	One beam energy	Peak irradiat. power	Beam spot diameter on target
197	1.96 ms	10 GeV	40 μs	10	1.0 MJ	2000 TW	2.2 mm

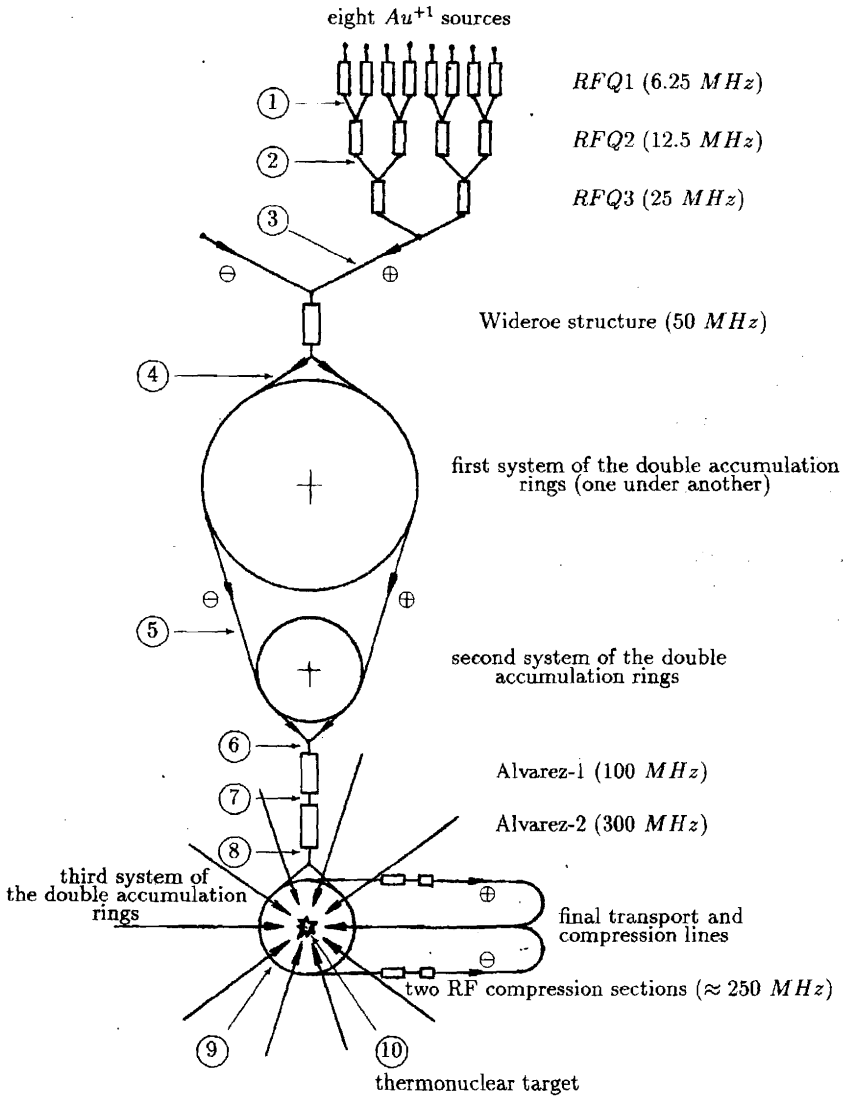

Figure 1: Sketch of driver layout

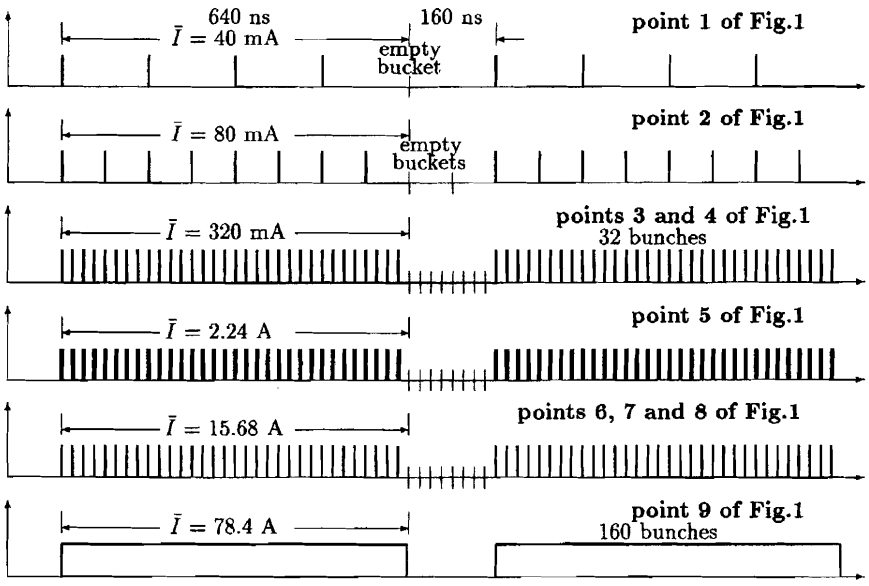

Figure 2: Ion bunch train evolution

Table 2: Parameters of beam at different stages in driver

Point of Fig.1	Energy T, GeV	Bunches freq., MHz	Momentum spread, $\pm\Delta p/p$	Emittance ε, $cm \cdot mrad$	β	Bunch length, cm	Bunch train current
1	0.015	6.25	$56 \cdot 10^{-4}$	2.4	0.0128	7.4	40 mA
2	0.05	12.5	$44 \cdot 10^{-4}$	1.3	0.0235	6	80 mA
3	0.1	50	$27 \cdot 10^{-4}$	0.93	0.0332	9	320 mA
4	0.6	50	$15 \cdot 10^{-4}$	0.41	0.0775	8.1	320 mA
5	0.6	50	$15 \cdot 10^{-4}$	0.67(v),8.3(h)	0.0775	8.1	2.24 A
6	0.6	50	$22.5 \cdot 10^{-4}$	13.4	0.0775	5.75	15.68 A
7	2.5	50	$9 \cdot 10^{-4}$	6.0	0.158	6.69	15.68 A
8	10	50	$7 \cdot 10^{-4}$	3.2	0.316	4.0	15.68 A
9	10	250	$4.7 \cdot 10^{-4}$	3.2	0.316	6.0	78.4 A
10	10	merged pulses	$\approx 8 \cdot 10^{-3}$	3.2	0.316	95	+5 kA, −5 kA

The beam is bunched beforehand at the entry of each first RFQ-linac sections with work frequency 6.25 MHz and the beam bunch structure is kept up down to the encounter with thermonuclear target. In this bunch train each fifth bucket-separatrix is an empty one. As a result the bunch train will have "holes" with duration $\simeq$ 160 ns and period 800 ns (see Fig. 2). Then all following operations of beam ejection and injection between some driver parts will not lead to any designed ion loss on vacuum chamber walls. Eight positive and eight negative current lines are planned. The absolute value of current is $\geq$ 40 mA in each line without the "hole" accounting. On the whole the linac complex is similar to the "classical" scheme of HIF driver. But so called "accumulation" rings (two for positive and two for negative current) are inserted in the linac structure (the point of transition from Wideroe to Alvarez linac) . These rings, in which of them the bunch beam structure is supported with help of the small amplitude RF field at frequency 100 MHz and the beam circulates not more then 7 turns not under final ion energy (10 GeV), but under intermediate one ($\simeq$ 600 MeV), are used for a compression in transversal co-ordinat space. Consequently, the bunch train duration in Alvarez is reduced by 49 times.

There are no limits on the beam current arising from instabilities and the Lasslet tune shift in accumulation rings contrary storage ones. Firstly, the beam dwelling time is very small here. Secondly, the beam parameters change from turn to turn, and there is no periodicity of motion which could lead to resonance or instabilities. The absence of Coulomb limits allows to maintain the beam bunch structure.

The compression in longitudinal co-ordinat space is realized in three stages. Eightfold compression is accomplished on score of the funnelling at the beginning of the linac complex. Next fivefold compression is produced in the third system of the double accumulation rings after that the bunch train frequency will be 250 MHz. Then the beam bunch trains (ten ones of positive and ten of negative ions) are ejected from third accumulation rings in twenty final transport and compression lines along ten directions with angle 36° between them. Each direction contains plus and minus branches. Here the last stage of longitudinal compression by 64 times is produced by two usual Alvarez sections with frequency $\simeq$ 250 MHz. After half of each this line the beams of the positive and negative ions are bent by 180° and merged, and then ten neutral beams propagate forwards the thermonuclear target. The beam energy of each channel is 1 MJ, the irradiation time is

$\approx 10\ ns$. The mean summary irradiation power is 1000 TW. The peak power attains 2000 TW.

2 Linear Accelerator

2.1 Injector

There are necessary 16 sources of single-charged Au ions. The sources are divided in two arrays according to the ion charge sign: eight sources of positive ions and eight sources of negative ions. All sources produce identical parallel beams: energy of 0.15 MeV, radius of 0.2 cm, transverse emittance 24 $cm \cdot mrad$ (emittance is not normalized and represents a square in coordinat $(x; x')$ divided by π). Each source must produce the entry separatrix bucket of the injector (momentum spread 17% and phase length 330°) with the average pulse current about $\geq 40\ mA$. The distance between beams in each array is 15 cm. The distance between arrays (middle axis) is 3.6 m The sources of each array are positioned symmetrically to common axis.

Each ion source is followed by its RFQ injector. That is that the injector part consists of two arrays (according to the sign of ions) with eight channels in each one [4]. All channels are located in one horizontal plane. Eight injector channels of each array may be placed in common vacuum volume and fed by common source of RF energy. The total length of RFQ injector is about 855 m, output energy is 100 MeV. The injector consists of three consequent RFQ accelerating channels (RFQ1, RFQ2, RFQ3) with different radio frequencies (RF). The main characteristics of the beam and RFQ channels are given in Table 3. The denominations are as follows: V - the voltage between the neighbour electrodes, L - channel length, N_p - number of structure periods (of length $\beta\lambda$), A - channel aperture, W - ion kinetic energy, β - ion velocity to light velocity ratio, $\lambda = c/RF$, φ_s - synchronous phase, $(\Delta p/p)_{sep}$ - momentum half spread of the separatrix, b - bunch length, $(\Delta p/p)_b$ - momentum half spread of the bunch, ε - emittance, a - maximum transverse beam size, m - modulation of the electrodes. If the electrode profile is $R(z) = (1 + \varepsilon \cos(2\pi z/\beta\lambda))$, where z is the longitudinal co-ordinate, then $m = (1 + \varepsilon)/(1 - \varepsilon)$.

The mismatching of the transverse and longitudinal oscillations due to jumps φ_s of RF is minimized as it is possible by suitable choice of channel characteristics in boundary points [4,5].

2.2 The main accelerator

The main accelerating channel consists of three stages. The first one is Wideroe accelerating structure, the second and the third ones are Alvarez drift tube accelerators (see Fig. 1). Data concerning the stages and the beam parameters are shown in Table 4. The denominations in this Table are: N_{tb} - the number of drift tubes, $\alpha = g/\beta\lambda$ - the gap coefficient, μ - the phase advance of transverse oscillations, G - the gradient of the magnetic field in quadrupoles, L_f - the focusing period, E - accelerating electric field. Initial part of each stage is a quarter-wave bunching device for matching of the longitudinal oscillations. The total length of main accelerator is 3200 m. For the focusing it is necessary 12500 quadrupoles of length from 20 cm to 50 cm. The gradient of the magnetic field in the quadrupoles is ranged from 1 kGs/cm to 5 kGs/cm. The necessary values of the magnetic induction on the edges of the aperture do not exceed 14 kGs. Some quadrupoles are supposed to be made of permanent magnets.

For the output beam the bunch length is 4 cm, the momentum spread $\pm 0.07\%$, maximum transverse emittance in both direction is about 3.2 $cm \cdot mrad$, maximum radius is about 2.3 cm, the bunches repetition frequency is 50 MHz, spatial bunches period $\approx$ 190 cm. Two Alvarez sections of the main accelerator need RF power of 150 GW for beam acceleration.

The presence of the large number of focusing and accelerating elements in the main channel essentially accentuate the importance of the question about the misalignments influence. According to the estimations, at the real tolerances on the accuracy of the manufacture and assembly of the accelerating channels the effective growth of the phase volumes achieves unacceptable values. Consequently, a system of the automatic correction of the beam parameters should be provided. For the beam consisted of bunches with charges of different signs this question demands special studying. Note that all forces disturbing the particles motion are of electromagnetic nature and hence are equal in value and opposite in direction for the ions of different signs. On the same reason the correcting fields calculated for the particles of one sign automatically will be valid for another signed particles also. This rule is not valid only for the defects of the injection in main accelerator as before it the ions of different signs move in different channels. The total growth of the longitudinal phase space along the linac is about 45%. The transverse phase volume in each direction increases in about 40%.

Table 3: Main injector parameters

value	unit	RFQ1		RFQ2		RFQ3	
RF	MHz	6.25		12.5		25	
V	kV	190		320		400	
L	m	122.4		277.6		406.5	
N_p		395		935		1363	
A	cm	1.47		1.44		1.44	
		entry	exit	entry	exit	entry	exit
W	MeV	0.150	15	15	50	50	100
$\beta \cdot 10^2$		0.128	1.28	1.28	2.35	2.35	3.32
$\beta\lambda$	cm	6.17	61.7	30.8	56.3	28.1	39.8
m		1.09	1.27	1.05	1.50	1.07	1.11
φ_s	degree	88.8	37	45	37	45	30
$(\Delta p/p)_{sep}$	$\pm\%$	17.4	1.13	0.73	1.02	0.59	0.30
b	cm	5.6	7.4	7.4	6.0	6.0	9.0
$(\Delta p/p)_b$	$\pm\%$	9.0	0.56	0.62	0.44	0.52	0.27
ε	$cm \cdot mrad$	24.1	2.4	2.4	1.3	1.3	0.93
a	cm	0.52	0.52	0.52	0.51	0.51	0.50

Table 4: Parameters of the main linear accelerator

value	unit	Wideroe		Alvarez 1		Alvarez 2	
		entry	exit	entry	exit	entry	exit
W	GeV	0.1	0.6	0.6	2.5	2.5	10
RF	MHz	50		100		250	
L	m	568		512		2027	
V	kV	200		—		—	
E	kV/cm	—		37		37	
$\beta\lambda$	cm	19.9	48.6	24.3	49.275	19.71	38.25
α		0.05		0.2		0.2	
φ	degree	37		37		37	
$N_t b$		3126		1348		7521	
$(\Delta p/p)_{sep}$	$\pm\%$	1.04	0.43	0.72	0.51	0.29	0.22
$(\Delta p/p)_b$	$\pm\%$	0.56	0.15	0.35	0.14	0.17	0.07
b	cm	5.2	8.1	3.7	4.3	3.4	4.0
ε	$cm \cdot mrad$	1.0	0.41	13.5	6.0	6.0	3.2
a	cm	1	0.48	2.3	2.3	2.3	2.3
μ	degree	6.8	40.5	45		45	
L_f		3		10		30	
G	kGs/cm	2.4	5.0	4.1	2.1	2.16	1.0
A	cm	3	1.5	3.45		3.45	

Table 5: Parameters of accumulation rings

Numb. of ring	Ion energy, GeV	Ring length, m	Mag. field mean val. kg	Revol. time, μs	Betatr. freq., Q_0	ΔQ_i	RF voltage, MV	RF frequency, MHz
1	0.6	6507	0.502	280	$\simeq 320$	84	391	100
2	0.6	929	3.49	40	$\simeq 100$	26	56	100
3	10	758	17.48	8	$\simeq 12$	9.6	218	250

3 Beam compression in the transversal space

The earlier proposed scheme of multiturn injection [2] is impossible here due to a high value of the betatron frequency shift ($\Delta Q \geq 1$). In the new concept two circumstances are used. Firstly, the dwelling time in the accumulation ring is short due to the small duration of the compression process (5-7 turns). Secondly, betatron oscillations of the beam center of gravity are little affected by Coulomb forces at the low image forces. All this allows to accumulate the beam by use of a bump with variable strength of the closed orbit distortion, in spite of a high value of Lasslet tune shift.

The emittance growth during such a multiturn injection is an important parameter. Let us denote the grow up factor by κ_i. The corresponding coefficient for the orthogonal degree of freedom will be denoted, as κ_{ort}. The resulting two dimensional blow up coefficient κ_r will be obviously equal to $\kappa_i \cdot \kappa_{ort}$.

The minimization of the κ_r value has been done numerically. The change of the injected beam shape as a function of the bump strength for $n > 2$ (n is the injection turn number) gives in the best case the result $\kappa_i = n^{1.5}$. For κ_{ort} we have found $\kappa_{ort} \simeq n^{\alpha}$, where $\alpha = \delta Q_{ort}/Q_0$, δQ_{ort} is the difference between the initial tune shift and the final one ($\delta Q_{ort} = |\Delta Q_i - \Delta Q_f|_{ort}$), Q_0 is number of coherent betatron oscillations in the accumulation ring. Practically, $\alpha \leq 0.25$. Consequently we get $\kappa_r = n^{1.5} \cdot n^{0.25} = n^{1.75}$. So, taking the acceptable growth of the beam phase volume as 30 times, we determine that number of injected turns must not exceed 7.

The first and second accumulation rings are placed at the beam transition from the Wideroe to the Alvarez structure (at the intermediate energy of 600 MeV). This design reduces the ring size by a factor of 4. The main parameters of the accumulation rings are given in Table 5.

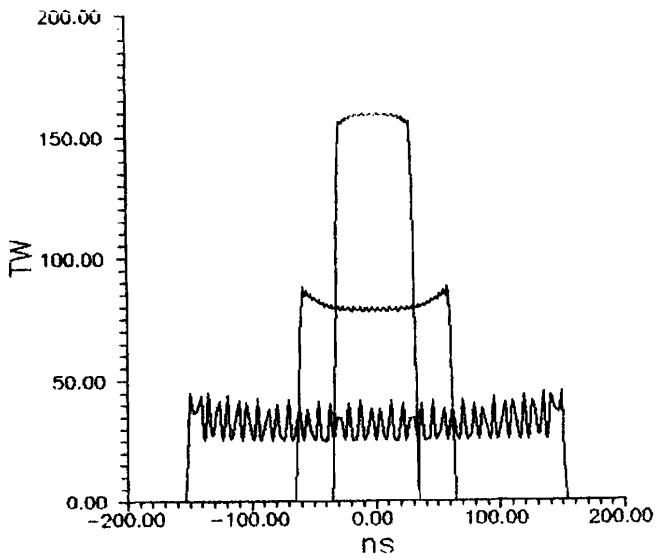

Figure 3: Pulse evolution on distance from the target 2000 m, 800 m, 400 m

4 Beam compression in the longitudinal space

The total longitudinal compression factor is equal to 2560. The mechanism of this compression is illustrated on Fig. 2. The evolution of the beam parameters during compression process both in longitudinal and transversal co-ordinat space is given in Table 2. In the initial part of the linac the mean beam current is increased by eight times both for Au^{+1} and Au^{-1} ions.

Then, at the final ion energy (10 GeV), the compression by a factor five is realized during five turns in the third system of the accumulation rings with the help of a periodic bump and a septum magnet (see point 9 of Fig. 1 on Fig. 2). The bump contains two deflectors, the distance between them is equal to half of the betatron wavelength. The frequency of deflectors RF voltage is suited to the bunch frequency at ring entrance ($F_0 = 50\ MHz$). The next condition for ring circumference, $l = \beta c/F_0(n \pm 1/5)$ will exactly provide the time shift between adjoining revolutions equal to $F_0^{-1}/5$. Such technique is described in detail in the papers [2] and, partly, in [6].

As a result we get 20 batches (10 of Au^{+1} ions and 10 of Au^{-1} ions)

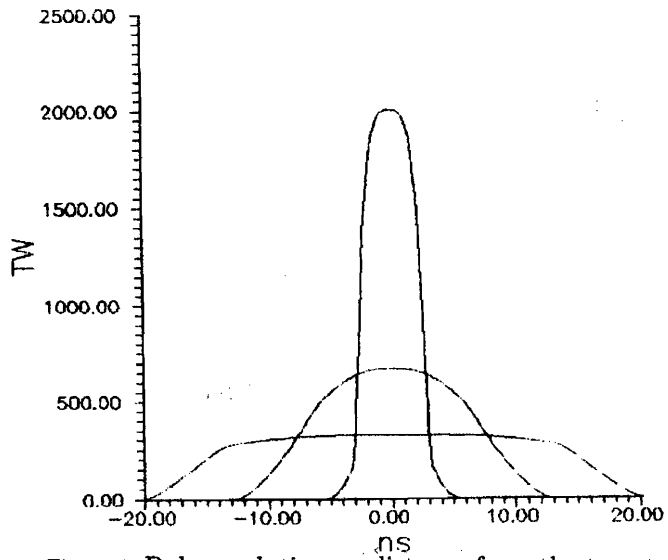

Figure 4: Pulse evolution on distance from the target 200 m, 100 m, 0 m

with a mean current of 78.4 A, duration of each batch is $\leq$ 640 ns and spacing $\geq$ 160 ns. These 20 batches are ejected by kicker-magnets into 20 transport channels, where they are bunched by two Alvarez sections (the distance between them is 230 m) with a frequency $\approx$ 250 MHz and a potential 300 MV (the first) and 18 MV (the second). For linearity of the RF voltage in the first section the second harmonic with potential 37 MV is added.

The full length of each transport channel is 4250 m. After half of this distance the beams of the positive and negative ions are bent by 180° and merged, and then ten neutral beams propagate forwards the thermonuclear target. So, a 64-fold final compression is realized in the transport channels and each of the trains of 160-bunches transforms into a single current pulse. The evolution of the batch has been investigated numerically. In Fig. 3 the shape of the pulses for the distance 2000 m, 800 m, 400 m from the target and in Fig. 4 for 200 m, 100 m, 0 m are given.

5 Transport and final focusing system

5.1 Linear theory results

Equations describing the coherent dipole and quadrupole oscillations of the two component heavy ion beams transported through periodical focusing channels have been obtained in linear approximation [7]. The conclusions can be summarized as the following.

- This method allows to increase essentially the ion current through the periodic focusing channel and, therefore, to upgrade the energy deposition into the target.
- To obtain higher currents one should use lower phase advance $\sigma_0 < 1$ (σ_0 is the phase shift in one period of the focusing structure for zero beam current). To transport conventional one component beam, we have to increase σ_0, that is quite opposite to transport of charge compensated beams.
- The circular frequency of noncoherent oscillation ω (in radians/period) is equal to the phase advance σ and increases rather slow when the current grows up (see Fig. 5). For one component ion beam transport this frequency strongly decreases when the current grows up, that is unlike again to charge compensated beams.
- The coherent quadrupole oscillations have two forms: the symmetrical mode and the antisymmetrical one. The circular frequency of coherent quadrupole oscillations for antisymmetrical mode σ_q^a grows rapidly with the beam current, unlike to one for symmetrical mode σ_q^s (equaled practically to double frequency of noncoherent oscillations). Beside that, σ_q^a is always bigger than the circular frequency of small dipole oscillations σ_d and is the biggest of the frequencies inherent in our system (see Fig. 5). Thus we conclude that this coherent quadrupole oscillations of antisymmetrical mode can be the most dangerous.
- When σ_q^a approaches to the boundary of quadrupole resonance band (the resonance condition is: $\sigma_q^a = 2\pi$), an instability occurs. This effect limits the beam current in periodic quadrupole focusing channel.

Fig. 5 demonstrates the dependence of coherent (σ_d, σ_q^a) and noncoherent (σ) frequencies from Coulomb parameter λ which is determined by the

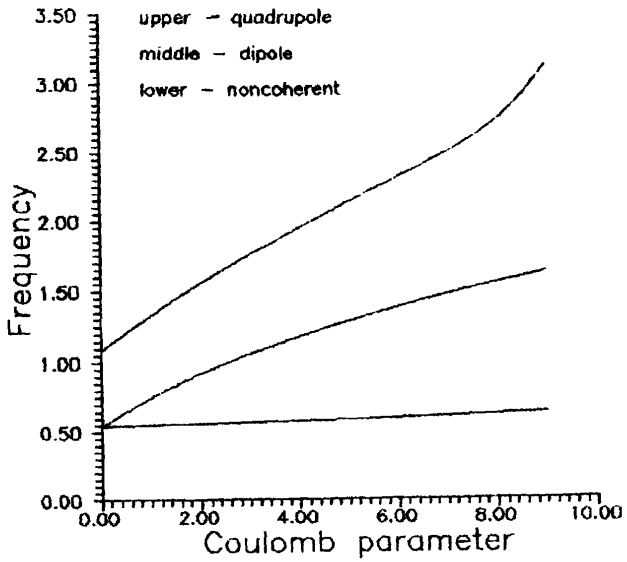

Figure 5: Dependence of $\sigma, \sigma_d, \sigma_q^a$ on λ

formula: $\lambda = QL/\varepsilon$. Here L is the length of one focusing period of the transport channel, ε is the beam emittance (the calculation was performed for $\varepsilon_x = \varepsilon_y = \varepsilon$). The Q is the beam perveance, determined by the formula:

$$Q = 4\frac{ZI}{AI_p(\beta\gamma)^3} \quad , \tag{1}$$

where Z and A are, respectively, the ion charge state and atomic number, I is the beam current of one component, I_p is Alfven current for protons ($I_p = 3.1 \cdot 10^4 kA$), β and γ are relativistic factors.

The current density for each beam component should be $\leq 1\ kA/cm^2$. This means, that the beam power (at the linac potential $\approx 10\ GV$) $\approx$ 200 TW per one channel can be easily transfered.

5.2 Intrinsic non-linear effects

Here we have studied non-linear effects, which couldn't be described in frames of K-V formalism. The tool for these studies is a particle simulation, which now seems to be the only way for quantitative estimate of charge

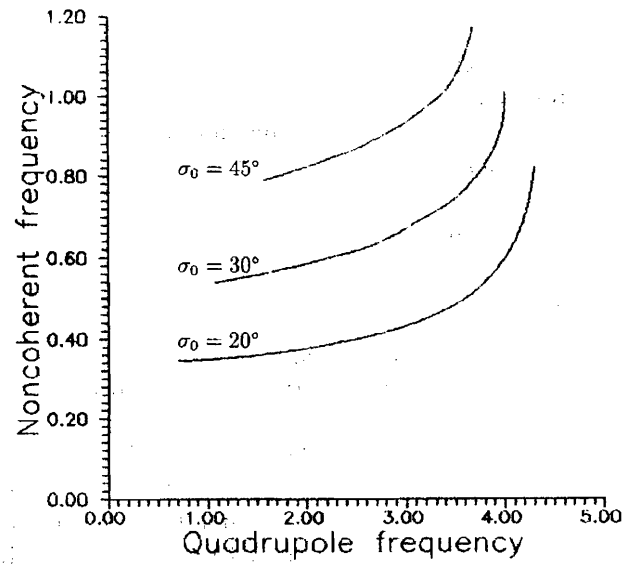

Figure 6: Dependence of σ on σ_q^a

compensated beams dynamics. There are no difficulties to adapt the usual 2D macro-particle algorithm for two-component beam simulation.

Thus, the found above envelopes and frequencies should be corrected by the general particle simulation. As a good initial approximation, we take beam parameters for K-V equations (which presents the exact solution for linear model) and test the beam motion during few n periods ($n \approx \pi/\sigma_q^s$) in periodical transport channel. Since the assigned beam envelopes are approximate (for non-linear case), we observe small oscillations due to mismatching. These oscillations occur nearby the *true* envelopes and mainly are the coherent quadrupole oscillations of symmetrical mode. The small component of the antisymmetrical mode may be neglected far off the resonance of quadrupole oscillations.

The amplitudes of envelope oscillations will be damped soon, due to strong intrinsic non-linearity of Coulomb forces, and we get the true values of the matched envelopes in the periodical channel. The emittance growth during this process is not critical ($\Delta\varepsilon/\varepsilon \approx 10^{-2}$) for our beam parameters: the total current 20 kA in two beam components, energy of ions (with

charge state $Z = 1$ and atomic number $A = 197$) 10 GeV, beam emittance 3.2 $cm \cdot mrad$.

However, the emittance growth depends on σ_q^a and becomes a critical for $\sigma_q^a \to 2\pi$, but we observe a significant growth of amplitudes earlier, when $\sigma_q^a \approx \pi$, because the resonance band is wide enough. We can conclude, therefore, that the condition $\sigma_q^a \leq \pi$ must be satisfied, that is in accordance to the results of linear theory. Fig. 6 demonstrates the frequencies of noncoherent betatron oscillations depending on quadrupole frequency σ_q^a.

5.3 Final focusing system

We should remember, that in the final focusing system (FFS) the condition $\sigma_q^a \leq \pi$ will be violated. Thus the FFS-part of the transport line should be considered separately from the periodical transport channels [8]. The input beam parameters at the FFS entrance should be matched to the output beam from the transport channel. A straight-forward and time-consumed way to find these FFS initial beam parameters if a detailed numerical simulation through the long transport line (about 100-150 periods). However, we can simplify the problem, assuming the initial beam is equal to the found above matched beam.

The final focusing system for the charge-compensation driver scheme has been investigated for the two-component ion (Au^{+1} and Au^{-1}) beam. Ion energy is 10 GeV. Calculations have been performed for beam current interval $1 \div 10$ kA for each beam component (total current $2 \div 20$ kA). Transverse beam emittance is $\varepsilon_H = \varepsilon_V = 3.2$ $cm{\cdot}mrad$, beam spot diameter on target is 2.2 mm, r.m.s. is 0.55 mm. Theoretical analysis has suggested that for the case of the beam charge compensation the longitudinal space charge effects have the third order of magnitude and can be neglected. Therefore, it is sufficient to use 2-dimensional macroparticle code in our calculations. Co-ordinates of macroparticles in phase space (x, p_x, y, p_y) are given by 4-dimensional transverse distribution. Calculations have been made for K-V distribution and, therefore, the region of non-linear space charge forces for one component is out of boundary of another component.

The following results have been obtained: the gradient of magnetic field in lenses is not more than 22 T/m (see Fig. 7), the radius of the beam cross-section in lenses is not more than 0.24 m (see Fig. 8), the distance between the beam focus point and the last lens of the focusing system is equal to 4 m, the length of the focusing objective is equal to 80 m.

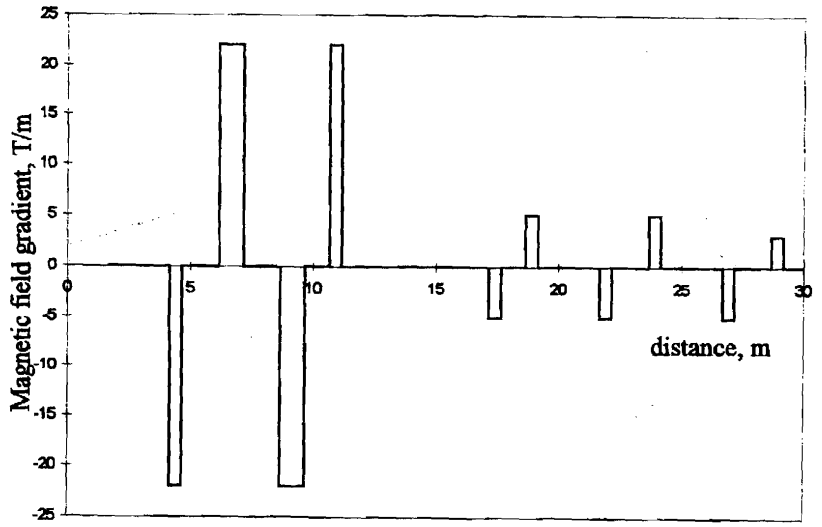

Figure 7: Final focusing system (F.F.S.)

Beam emittance grows along the structure has been calculated. The noticeable emittance growth in the final focusing system is caused by the big non-linearity of the space charge forces due to big difference of the beam component envelops that occurs in the focusing objective lenses. This effect arises from the big optical force of the final focusing system. For the total beam current 20 kA we have the emittance growth near 4%. Notice that this emittance growth is small enough and does not modify substantially the beam focusing spot size.

Study of non-linear effects in charge compensated ion beam confirms the validity of the next formula for the upper limit of the beam current:

$$I \leq \frac{\pi^2 A \varepsilon I_p}{4|Z|L\sigma_0}(\beta\gamma)^3(1 - \frac{4\sigma_0^2}{\pi^2}) \quad , \tag{2}$$

what it was shown in [7]. In the region $0.1 < \sigma_0 < 1$ (in radians) this formula gives good numerical results for beam current values. Note, that for $\sigma_0 \to 0$ the beam current tends to infinity just as the size of the beam cross-section.

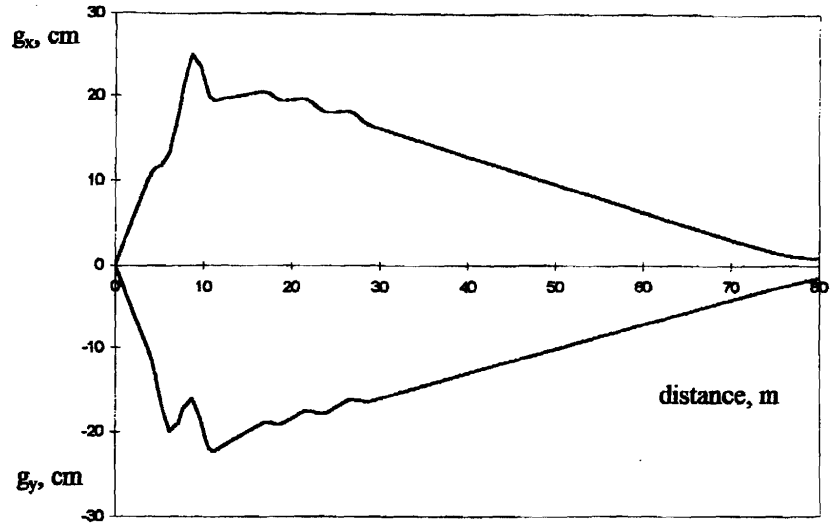

Figure 8: Ion beams envelopes (g_x, g_y)

6 Estimation of ion losses

The ion beams, used in the proposed driver scheme, should be stable enough. The total ion losses should not exceed 1% during the processes of acceleration, accumulation and beam transport.

There are three main reasons of ion losses: the ion scattering on the residual gas, the inter-beam scattering, and the spontaneous electron losses by negative ions due to the strong external electric field. The corresponding ion lifetime τ as a function of the electric field is given by

$$\log \tau = -13.17 - \log g + 0.5 \cdot \log E + 29.67 \cdot E^{3/2} \cdot g^{-1} \quad , \qquad (3)$$

where g is the electron-affinity energy (eV), τ is the lifetime in seconds, $E(MV/cm)$ is the external electric field in the ion rest system. A magnetic field $H(T)$ in the laboratory system corresponds to the electric field $E(MV/cm) = 3\beta\gamma \cdot H(T)$ in the ion rest system. The high energy g means that we can use high enough magnetic field in the accumulation rings without considerable ion losses. If we take $\tau \approx 1$ s then the corresponding H value for the Au ions ($g = 2.31$ eV) will be ≈ 7.5 T and the losses due to

this effect will be less 10^{-5}.

The scattering cross-section on the residual gas is practically the same for the negative and positive ions (under the assumption that the ion charge states are far from the equilibrium state), so it is not new limit on the residual gas pressure arise in this driver scheme.

As regards to inter-beam scattering, we can use the preliminary experimental data for the following charge-exchange reaction: $Au^{+1} + Au^{-1} \rightarrow Au^0 + ... \quad \sigma \approx 4 \cdot 10^{-15}\ cm^2$.

This reaction was investigated experimentally at the relative ions energy $10 - 100\ keV$. We can use the cross-section value from this reaction. The maximum ion losses δ in the magnetic ring due to the inter-beam scattering can be represent in the form

$$\delta = \frac{N \cdot \sigma \cdot v \cdot \varepsilon \cdot \tau}{8\pi^2 \cdot R^3 \cdot b} \quad , \tag{4}$$

where N is number of ions of one bunch,

σ is cross-section of the of inelastic ion-ion collision,

v is the ion bunch velocity,

ε is the beam emittance,

τ is the beam dwelling time,

R is the beam envelope radius,

b is the bunch length.

In our case $\delta \leq 2 \cdot 10^{-3}$ for each accumulation ring.

According to our investigation of the loss processes, which take place for some elements of the charge-symmetric driver with the beam neutralization, we have concluded that these processes are not dangerous but must be taken into account for driver resign.

Upon the whole the maximal ion losses for proposed driver scheme will not exceed $5 \cdot 10^{-3}$.

7 Conclusion

In conclusion note some questions which should be additionally considered during the following studies:

- The high loading problem of Alvarez linac (current $\simeq 15\ A$) needs to consider the possibility to use the sequence of superconducting resonators fed by high-power generators as a new linac structure.

- The problem of working out the intensive ($\simeq 50\ mA$) source of negative Au ions with the value of invariant emittance $\leq 10^{-2}\ cm \cdot mrad$ demands some attention and efforts in spite of the theoretical considerations already indicates the opportunity of such source creation.
- The process of multiturn injection in accumulation rings under high value of Coulomb tune shift should be studied more carefully including the computer simulation.
- The influence of the beam coupling on the beam emittance value during accelerating process and under opposite signed beams merging in the final channel should be calculated more precise.
- The usual value of chromatics of final beam transport channel (under beam momentum spread $\pm 8 \cdot 10^{-3}$ and beam spot radius on target 1.1 mm) is offered as inadmissibly high one. The possibility to create the almost achromatic transport channel should be considered in future.

8 Acknowledgement

This work has been performed in frames of the grant ISTC-154.

References

[1] D.G.Koshkarev,Nuovo Cimento 106 A, N11 (1993), 1567-1573.

[2] M.M.Basko,M.D.Churazov,D.G.Koshkarev,Fus.Eng.Des., 32-33,1996,73-85.

[3] D.G.Koshkarev,A.V.Barkhudaryan,A.N.Talyzin, 12-th HIF Symposium, September 24-27 1997, Heidelberg,Germany.

[4] M.I.Kapchinsky, I.L.Korenev, L.A.Yudin, D.G.Koshkarev, Fus.Eng.Des.,32-33,1996,355.

[5] D.G.Koshkarev-ITEP,L.A.Yudin,I.L.Korenev, S.V.Vinogradov MRTI RAN, Conceptual Design of Linac for Power HIF Driver.XVIII Intern.Linac Conf.,Geneva,Switzerland,26-30 Aug.,1996.

[6] D.G.Koshkarev, DESY, July 1995 TESLA 95-16.

[7] A.V.Barkhudaryan,D.G.Koshkarev,A.N.Talyzin. HIF Symposium, September 1995, Princeton,New Jercey,USA.

[8] A.V.Barkhudaryan,D.G.Koshkarev,L.G.Vorobiev. EPAC-96, v.2, p.1400, June 10-14 1996, Barcelona,Spain.

Д.Г.Кошкарев и др.

Новая концепция Зарядо-Симметричного Драйвера для ТИС.

Подписано к печати 25.03.98 Формат 60x90 I/I6
Усл.-печ.л.I,25. Уч.-изд.л.0,9. Тираж 9I экз. Заказ 5.
Индекс 3649

Отпечатано в ИТЭФ, II7259, Москва, Б.Черемушкинская, 25